Adaptive Passivity-Based Control of PEM Fuel Cell/Battery Hybrid Power Source for Stand-Alone Applications

Ali TOFIGHI, Mohsen KALANTAR
Center of Excellence for Power System Automation and Operation,
Department of Electrical Engineering, Iran University of Science and Technology, Tehran, Iran
tofighi@iust.ac.ir, kalantar@iust.ac.ir

[1]***Abstract*—In this paper, a DC hybrid power source composed of PEM fuel cell as main source, Li-ion battery storage as transient power source and their power electronic interfacing is modelled based on Euler-Lagrange framework. Subsequently, adaptive passivity-based controllers are synthesized using the energy shaping and damping injection technique. Local asymptotic stability is insured as well. In addition, the power management system is designed in order to manage power flow between components.**

Evaluation of the proposed system and simulation of the hybrid system are accomplished using MATLAB/Simulink. Afterwards, linear PI controllers are provided for the purpose of comparison with proposed controllers responses. The results show that the outputs of hybrid system based on adaptive passivity-based controllers have a good tracking response, low overshoot, short settling time and zero steady-state error. The comparison of results demonstrates the robustness of the proposed controllers for reference DC voltage and resistive load changes.

***Index Terms*—Adaptive Passivity-Based Control, Batteries, Fuel Cells, Hybrid power systems, Load management**

I. INTRODUCTION

Distributed Generation (DG) has the advantages of low investment, low pollution, high efficiency, and high reliability. Fuel cells (FCs) are mostly being used due to some merits compared to the other types of DG sources [1]. However, one main disadvantage of fuel cell is its slow dynamics [2]. Hence, hybrid power sources are introduced to make the best use of its advantages and elimination of the aforementioned disadvantage [3-5]. Batteries are a secondary source which can supply power under transient conditions [6].

Fuel cells act as converters which convert the chemical energy into electrical energy [7]. Proton Exchange Membrance (PEM) fuel cell is a prime candidate for hybrid systems, because it has higher power density and lower operating temperature than the other types of FC systems [8].

Power electronic converters have a significant role in the hybrid systems [9]. These are interface between the DG sources and the other parts of hybrid system [7, 10]. Recently, some of researchers have concerned on control of hybrid power sources [11-13]. The methods of controller design classifies into two categories: linear and nonlinear. The linear methods performed relying on locally linearized models. Hence, their performance will not remain the same under any changes on equilibrium points. The PI controller is a main linear controller which is being used in DG applications [14-17]. The dynamic equations of the power electronic converters have a nonlinear nature due to the multiplications of the state variables by the control inputs [18]. Therefore, the nonlinear methods such as robust [19], feedback linearization [20], sliding mode [21] and passivity-based control [22] are used for control of converters. In particular, a passivity-based control method has taken into consideration in various industrial applications.

The Passivity-Based Control (PBC) was introduced, by Ortega et al., as a controller design methodology which achieves stabilization by passivation [23]. Two theories for PBC were developed which are: Euler-Lagrange (EL)-PBC [24, 25] and Interconnection and Damping Assignment (IDA)-PBC [23]. These methods have been mostly used for control of induction motors [26], and switching power converters [27, 28].

Lee has used EL-PBC for control of three phase AC/DC voltage source converter [29]. Also, a single phase PWM current source inverter control with applying IDA-PBC has been implemented by Komurcugil [30]. The control of DG hybrid systems based on the IDA-PBC is achieved [31].

In the most of hybrid systems, the value of the resistive load is constant but unknown. Therefore, adaptive type of controllers has been used to handle this type of uncertainty. Sira-Ramirez et al., has developed adaptive input-output linearization controller [32], and adaptive passivity based controller [33] for DC/DC converters.

The study in this paper is concentrated on the lagrangian modeling of the fuel cell/battery DC hybrid power source, which the fuel cell is a main power source and battery storage is used as a transient power source. The control signals are achieved by Adaptive PBC (APBC). Power flow between hybrid system components is managed in the power management unit.

The paper is organized as follows. Section II introduces the hybrid DC power source and explains the suitable model of each component which is applied on hybrid system. Section III presents Euler-Lagrange model of DC hybrid power source. Adaptive Passivity-Based Controllers design is achieved in section IV Linear PI controllers are provided in section V for comparison with proposed system. Section VI describes power management system. Section VII validates the proposed model by simulation results and section VIII concludes the paper.

Digital Object Identifier 10.4316/AECE.2010.04018

II. PROPOSED SYSTEM DESCRIPTION

The proposed hybrid power source is depicted in Fig. 1. This power source consists of a PEM fuel cell, Li-ion battery storage, DC/DC converter, passivity-based controllers, load, and a power management center.

A. PEM Fuel Cell Dynamic Model

A fuel cell is a static energy conversion device that converts chemical reaction of fuels directly into electrical energy. This energy conversion occurs whenever a fuel (hydrogen-rich gas) reacts chemically with the oxygen of air [3].

The PEMFC stack voltage is a function of Nernst's voltage, activation, concentration and ohmic losses. Therefore, the FC output voltage is expressed as:

$$V_{Cell} = E_{Nernst} - V_{act} - V_{ohm} - V_{con} \quad (1)$$

Where $V_{Cell}, E_{Nernst}, V_{act}, V_{Ohmic}, V_{Conc}$ are FC stack, Nernst, activation, ohmic and concentration voltage, respectively.

The Nernst's voltage is written as:

$$E_{Nernst} = N(E_0 + \frac{RT}{2F} Ln[P_{H_2}.P_{O_2}^{\frac{1}{2}}]) \quad (2)$$

Where N is the Number of cells, E_0 is cell no load voltage, R is universal gas constant, T is temperature, F is Faraday constant, and P_{H_2}, P_{O_2} are hydrogen and oxygen partial pressures.

Activation voltage drop is calculated by Tafel equation [1]. Its equation is divided into two terms, the first term (V_{act1}) is the drop voltage affected only by the fuel cell operating temperature [1]:

$$V_{act1} = \eta_0 + (T - 298).a \quad (3)$$

Where η_0 is the temperature invariant part of V_{act1} and a is constant.

The second term (V_{act2}) depends on both current and temperature [1]:

$$V_{act2} = T.bLn(I) \quad (4)$$

Where b is constant.

The equivalent resistance of activation (R_{act}) found by dividing V_{act2} with the cell current density. The ohmic resistance of a PEM fuel cell is defined in two parts.

The first part is due to the transfer of electrons through the electrodes and the other part is due to the transfer of protons through the membrance [3]. Therefore, the ohmic voltage drop is as follows:

$$V_{Ohmic} = IR_{Ohmic} = I(R_M + R_C) \quad (5)$$

Where R_C is the electrodes resistance which is a constant parameter. The equivalent resistance that protons pass the membrance (R_M) is defined as [3]:

$$R_M = \frac{\rho_M l}{A} \quad (6)$$

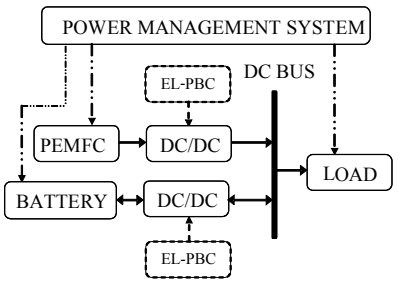

Fig. 1. Structure of proposed DC hybrid power source.

Where A is the cell active area; l and ρ_M are membrance thickness and membrance specific resistivity, respectively which is expressed by [3]:

$$\rho_M = \frac{181.6[1 + 0.03(I/A) + 0.062(T/303)^2 (I/A)^{2.5}]}{[\varphi - 0.634 - 3(I/A)e^{(4.18(T - \frac{303}{T}))}]} \quad (7)$$

Where φ is an adjustable parameter with a maximum value of 23.

The last term of FC voltage is the concentration voltage drop. It is mainly due to the reactive concentration excess near the catalyst surfaces which is defined as [1]:

$$V_{Conc} = -B.Ln(1 - \frac{J}{J_{\max}}) \quad (8)$$

Where B is constant parameter and J is current density which is expressed as:

$$J = \frac{I}{A} \quad (9)$$

The equivalent resistance for the concentration loss is:

$$R_{Conc} = -\frac{B}{I}.Ln(1 - \frac{J}{J_{\max}}) \quad (10)$$

The dynamic characteristic of PEM fuel cell is called 'double layer charging effect' [1]. In the fuel cell, the layer of electrodes and the electrolyte acts as a charging surface that they store the electrical charges and energy as a capacitor.

Therefore, this phenomenon is modelled like a capacitor and added to the PEM fuel cell model. Considering the aforementioned expressions, the equivalent circuit of dynamic model of PEMFC is presented in Fig. 2.

The voltage across capacitor in PEMFC model is [1]:

$$V_C = (I - C\frac{dV_C}{dt})(R_{act} + R_{conc}) \quad (11)$$

The cell voltage (1) is represented as:

$$V_{out} = E - V_C - V_{act1} - V_{Ohmic} \quad (12)$$

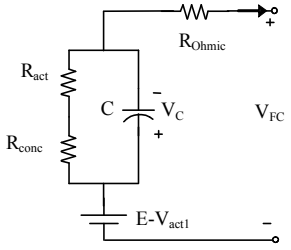

Fig. 2. PEM fuel cell dynamic electric model [1].

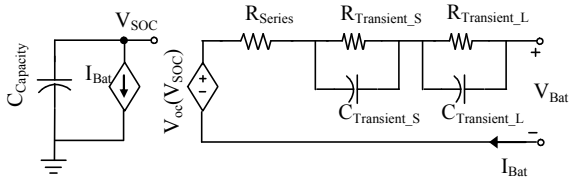

Fig. 3. Battery circuit model [37].

B. *Lithium-Ion Battery Model*

Storage devices are used as energy storing in the hybrid power sources [34, 35]. The batteries store energy in the electrochemical form. Li-ion batteries are preferable to other types of batteries because they have high energy density, high operating voltage levels and long cycle life [36].

In this section, the dynamic model of Li-ion battery is introduced which is used in the simulation program. Chen and Mora [37] proposed a suitable model for Li-ion battery which predicts battery runtime and I-V performance accurately. The aforementioned model of the Li-ion battery is depicted in Fig. 3.

The model consists of two separate circuits linked by a voltage-controlled voltage source and a current-controlled current source. The runtime and State Of Charge (SOC) of the battery is calculated by using left side circuit. The equivalent internal impedance simulates the internal resistance and transient behavior of the battery. Hence, R_{Series} is responsible for voltage drop in battery voltage, and the components of the RC networks are responsible for short and long-time transients in the battery internal impedance. The elements of the equivalent internal impedance are a function of SOC, and can be achieved as:

$$\begin{aligned}
R_{Series}(SOC) &= 0.1562e^{-24.375\cdot SOC} + 0.07446 \\
R_{Transient_S}(SOC) &= 0.3208e^{-29.14\cdot SOC} + 0.04669 \\
C_{Transient_S}(SOC) &= -752.9e^{-13.51\cdot SOC} + 703.6 \\
R_{Transient_L}(SOC) &= 6.603e^{-155.2\cdot SOC} + 0.04984 \\
C_{Transient_L}(SOC) &= -6056e^{-27.12\cdot SOC} + 4475 \\
V_{OC}(SOC) &= -1.031e^{-35\cdot SOC} + 3.685 + 0.2156\cdot SOC - \\
&\quad 0.1178\cdot SOC^2 + 0.3201\cdot SOC^3 \\
SOC(t) &= SOC(0) - \frac{1}{C_{Cap}}\int_0^t i(\tau)d\tau
\end{aligned} \tag{13}$$

C. *DC/DC converter*

The amplitude of DC output voltage of the fuel cell depends on both the internal electrochemical reaction and the external load impedance. Therefore, the boost DC/DC converter is used to regulate the output voltage of the fuel cell. Also, a bidirectional DC/DC converter is used to control the charging and discharging of the battery storage. The boost DC/DC converter is depicted in Fig. 4.

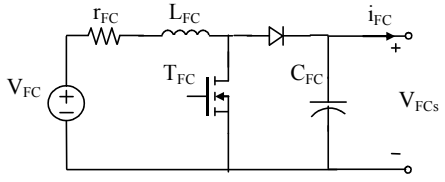

Fig. 4. Boost DC/DC converter.

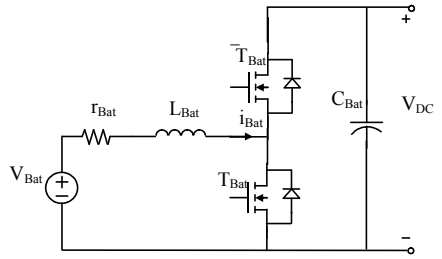

Fig. 5. Bidirectional DC/DC converter.

The bidirectional DC/DC converter is an interface between the load and the battery storage which is depicted in Fig. 5. These converters are linked by DC inductor (L_{DL}).

III. Euler-Lagrange Model of the Hybrid Power Source

The overall structure of hybrid system is depicted in Fig.1. In the previous sections, a suitable model for DC/DC converters and other components have been presented. In this section, the EL description of them is expressed.

The Lagrangian $L(\dot{q},q)$ of the system is the difference of the magnetic co-energy of the inductive elements, denoted by $T(\dot{q},q)$, and the electric field energy of the capacitive elements, denoted by $V(q)$, i.e.

$$L(\dot{q},q) = T(\dot{q},q) - V(q) \tag{14}$$

Where q is the vector of the electric charges and $\dot{q}$ is the vector of the flowing current. The EL modeling equations with consideration of circuit constraints is [25]:

$$\begin{aligned}
&\frac{d}{dt}\left(\frac{\partial L}{\partial \dot{q}}(\dot{q},q)\right) - \frac{\partial L}{\partial q}(\dot{q},q) = -\frac{\partial D}{\partial \dot{q}}(\dot{q}) \\
&\qquad + A(q)\lambda + F_q \\
&A(q)^T\dot{q} = 0
\end{aligned} \tag{15}$$

Where $D(\dot{q})$ is the Rayleigh dissipation function, and F_q is the vector of generalized forcing functions.

In our case, the elements of the vector q, $\dot{q}$ consist electric charges q_{C_FC}, q_{C_Bat}, and $\dot{q}_{L\_FC}$, $\dot{q}_{L\_Bat}$, $\dot{q}_{L\_DC}$ corresponding to the fuel cell and battery DC/DC converter capacitors, and fuel cell, battery DC/DC converters and DC link inductors, respectively.

In the view of the hybrid system configuration represented in Fig. 2-5, the following EL equations:

$$T = \frac{1}{2}(L_{FC}\dot{q}^2_{L\_FC} + L_{Bat}\dot{q}^2_{L\_Bat} + L_{DC}\dot{q}^2_{L\_DC}) \tag{16}$$

$$V = \frac{1}{2}\left(\frac{1}{C_{FC}}q^2_{C\_FC} + \frac{1}{C_{Bat}}q^2_{C\_Bat}\right) \tag{17}$$

$$\begin{aligned}
D &= \frac{1}{2}r_{FC}\dot{q}^2_{L_FC} + \frac{1}{2}r_{Bat}\dot{q}^2_{L_Bat} \\
&\quad + \frac{1}{2}R_L\left[(1-u_{Bat})\dot{q}_{L_Bat} + \dot{q}_{L_DC} - \dot{q}_{C_Bat}\right]^2
\end{aligned} \tag{18}$$

$$F_q = \begin{bmatrix} V_{FC} & V_{Bat} & 0 & 0 & 0 \end{bmatrix}^T \tag{19}$$

Where r_i and L_i is resistance and inductance of boosting inductor, respectively and C_i is the capacity of the DC side filter capacitor, which $i = FC, Bat$ denote the fuel cell and battery DC/DC converter, R_L is load resistance.

The constraint equations are given by the Kirchhoff's current law, hence, the constraint matrix will be:

$$A = \begin{bmatrix} -(1-u_{FC}) & 0 & 1 & 1 & 0 \end{bmatrix}^T \tag{20}$$

With definition $q = \begin{bmatrix} q_{L\_FC} & q_{L\_Bat} & q_{L\_DC} & q_{C\_FC} & q_{C\_Bat} \end{bmatrix}^T$ and considering (15) and (20), the EL equations are expanded as a set of scalar differential equations.

$$\frac{d}{dt}\left(\frac{\partial L}{\partial \dot{q}_{L\_FC}}\right) - \frac{\partial L}{\partial q_{L\_FC}} = -\frac{\partial D}{\partial \dot{q}_{L\_FC}} - (1-u_{FC})\lambda + V_{FC} \tag{21}$$

$$\frac{d}{dt}\left(\frac{\partial L}{\partial \dot{q}_{L\_Bat}}\right) - \frac{\partial L}{\partial q_{L\_Bat}} = -\frac{\partial D}{\partial \dot{q}_{L\_Bat}} + V_{Bat} \tag{22}$$

$$\frac{d}{dt}\left(\frac{\partial L}{\partial \dot{q}_{L\_DC}}\right) - \frac{\partial L}{\partial q_{L\_DC}} = -\frac{\partial D}{\partial \dot{q}_{L\_DC}} + \lambda \tag{23}$$

$$\frac{d}{dt}\left(\frac{\partial L}{\partial \dot{q}_{C\_FC}}\right) - \frac{\partial L}{\partial q_{C\_FC}} = -\frac{\partial D}{\partial \dot{q}_{C\_FC}} + \lambda \tag{24}$$

$$\frac{d}{dt}\left(\frac{\partial L}{\partial \dot{q}_{C\_Bat}}\right) - \frac{\partial L}{\partial q_{C\_Bat}} = -\frac{\partial D}{\partial \dot{q}_{C\_Bat}} \tag{25}$$

After a straightforward calculation of (21-25) with the EL parameters (16-20), the EL model equations are yielded in the following form:

$$L_{FC}\ddot{q}_{L\_FC} + r_{FC}\dot{q}_{L\_FC} + (1-u_{FC})\frac{1}{C_{FC}}q_{C\_FC} = V_{FC} \tag{26}$$

$$L_{Bat}\ddot{q}_{L\_Bat} + r_{Bat}\dot{q}_{L\_Bat} + (1-u_{Bat})\frac{1}{C_{Bat}}q_{C\_Bat} = V_{Bat} \tag{27}$$

$$L_{DC}\ddot{q}_{L\_DC} - \frac{1}{C_{FC}}q_{C\_FC} + \frac{1}{C_{Bat}}q_{C\_Bat} = 0 \tag{28}$$

$$-(1-u_{FC})\ddot{q}_{L\_FC} + \dot{q}_{L\_DC} + \dot{q}_{C\_FC} = 0 \tag{29}$$

$$(1-u_{Bat})\ddot{q}_{L\_Bat} + \dot{q}_{L\_DC} - \dot{q}_{C\_Bat} - \frac{1}{R_L C_{Bat}}q_{C\_Bat} = 0 \tag{30}$$

Which results with $z = \begin{bmatrix} i_{FC} & i_{Bat} & i_{DC} & V_{FCs} & V_{DC} \end{bmatrix}^T$ $= \begin{bmatrix} \dot{q}_{L\_FC} & \dot{q}_{L\_Bat} & \dot{q}_{L\_DC} & \frac{1}{C_{FC}}q_{C\_FC} & \frac{1}{C_{Bat}}q_{C\_Bat} \end{bmatrix}^T$ in the state equation:

$$L_{FC}\dot{z}_1 + r_{FC}z_1 + (1-u_{FC})z_4 = V_{FC} \tag{31}$$

$$L_{Bat}\dot{z}_2 + r_{Bat}z_2 + (1-u_{Bat})z_5 = V_{Bat} \tag{32}$$

$$L_{DC}\dot{z}_3 - z_4 + z_5 = 0 \tag{33}$$

$$C_{FC}\dot{z}_4 - (1-u_{FC})z_1 + z_3 = 0 \tag{34}$$

$$C_{Bat}\dot{z}_5 - (1-u_{Bat})z_2 - z_3 + \frac{z_5}{R_L} = 0 \tag{35}$$

The aforementioned equations represent in the matrix form as:

$$M\dot{z} + T(u)z + Rz = E \tag{36}$$

$$M = diag\{L_{FC};\ L_{Bat};\ L_{DC};\ C_{FC};\ C_{Bat}\}$$

$$R = diag\left\{r_{FC};\ r_{Bat};\ 0;\ 0;\ \frac{1}{R_L}\right\}$$

$$T = \begin{bmatrix} 0 & 0 & 0 & 1-u_{FC} & 0 \\ 0 & 0 & 0 & 0 & 1-u_{Bat} \\ 0 & 0 & 0 & -1 & 1 \\ -(1-u_{FC}) & 0 & 1 & 0 & 0 \\ 0 & -(1-u_{Bat}) & -1 & 0 & 0 \end{bmatrix} \tag{37}$$

$$E = diag\{V_{FC};\ V_{Bat};\ 0;\ 0;\ 0\}$$

Where M is a positive-definite diagonal matrix, T is the interconnection matrix, R is the dissipation matrix, and E is the vector consisting of voltage sources. The total energy function is:

$$H(t) = T + V = \frac{1}{2}z^T M z \tag{38}$$

Where satisfies the energy balance equation:

$$H(T) - H(0) + \int_0^T z^T R z dt = \int_0^T z^T E\, dt \tag{39}$$

Which describes that the sum of the stored energy and dissipated energy equals the supplied energy.

The control objective for this hybrid system is a DC value of the output voltage of both DC/DC converters equal to a DC bus constant voltage.

Substitute $z_{4d} = z_{5d} = V_d$ in the dynamical equations (31-35) after some calculations the equilibrium vector is expressed as:

$$z_d = \begin{bmatrix} z_{1d} & z_{2d} & z_{3d} & z_{4d} & z_{5d} \end{bmatrix}^T \tag{40}$$

In which $z_{id}, i = 1,2,...,5$, denote the desired constant equilibrium states of the closed loop system. Where

$$z_{1d} = \frac{1}{2r_{FC}}\left[V_{FC} - \sqrt{V_{FC}^2 - 4r_{FC}V_d z_{3d}}\right]$$

$$z_{2d} = \frac{1}{2r_{Bat}}\left[V_{Bat} - \sqrt{V_{Bat}^2 - 4r_{Bat}V_d\left(\frac{V_d}{R_L} - z_{3d}\right)}\right] \tag{41}$$

With suitable assuming for z_{3d} equilibrium point, z_{1d} and z_{2d} can be achieved from (41).

IV. Adaptive Passivity-Based Controller Design

It is assumed that the resistive loads of hybrid system are constant, but are unknown. Therefore, to handle this type of uncertainty, adaptive passivity-based control is developed, on the other hands, the main objective is the load supplying only by the DC source. Therefore, the DC/DC converter of fuel cell is controlled to maintain the DC bus voltage to a constant value. The battery storage has been considered for instantaneous loads and whenever the load power exceeds the fuel cell rated power. Hence, in this condition, the DC bus voltage will be constant with controlling of DC/DC converter of battery storage.

The resistive load can be estimate by adaptation approach. Let

$$\frac{1}{R_L} = \theta, \quad \tilde{\theta} = \hat{\theta} - \theta \tag{42}$$

Where $\hat{\theta}$ is the estimation value of θ, $\tilde{\theta}$ is the estimation error.

Also, consider the error state vector:

$$\tilde{z} = \begin{bmatrix} \tilde{z}_1 & \tilde{z}_2 & \tilde{z}_3 & \tilde{z}_4 & \tilde{z}_5 \end{bmatrix}^T$$

$$= \begin{bmatrix} z_1 - z_{1d} & z_2 - z_{2d} & z_3 - z_{3d} & z_4 - z_{4d} & z_5 - z_{5d} \end{bmatrix}^T$$

The error dynamic equation is expressed as:

$$M\dot{\tilde{z}} + T(u)\tilde{z} + R\tilde{z} = E - (M\dot{z}_d + T(u)z_d + Rz_d) \tag{43}$$

Adding $R_a\tilde{z}$ to both sides of equations (43), the error dynamics with desired damping is:

$$M\dot{\tilde{z}} + T(u)\tilde{z} + R_d\tilde{z} = E - (M\dot{z}_d + T(u)z_d + Rz_d - R_a\tilde{z}) \tag{44}$$

By considering the following desired error dissipation matrix:

$$R_d = R + R_a \tag{45}$$

Where R from (37) rewritten as:

$$R = diag\{r_{FC};\ r_{Bat};\ 0;\ 0;\ \hat{\theta}\} \tag{46}$$

Where the injected damping

$$R_a = diag\{r_{a1};\ r_{a2};\ 0;\ 0;\ 0\} \tag{47}$$

Supposing that the right-hand side of the equation (44) is:

$$M\ \dot{\tilde{z}} + T\ (u)\tilde{z} + R_d\ \tilde{z} = \psi \tag{48}$$

Where

$$\psi = E - (M\ \dot{z}_d + T\ (u) z_d + R z_d - R_a \tilde{z}) \tag{49}$$

Consider the total energy, (50), where γ is the strictly positive constant, as a Lyapunov function:

$$H_d(t) = \frac{1}{2}\tilde{z}^T M\ \tilde{z} + \frac{1}{2\gamma}\tilde{\theta}^2 \tag{50}$$

For (50) the asymptotic stability of the error dynamic is achieved due to the positive definiteness of the matrix M and satisfying its derivative:

$$\begin{aligned} \dot{H}_d(t) &= \tilde{z}^T M\ \dot{\tilde{z}} + \frac{1}{\gamma}\tilde{\theta}\dot{\tilde{\theta}} = -\tilde{z}^T R_d \tilde{z} \\ &+ \left[(z_4 - z_{4d})z_{5d} + (z_5 - z_{5d})z_{5d} + \frac{1}{\gamma}\dot{\tilde{\theta}}\right]\tilde{\theta} \end{aligned} \tag{51}$$

Hence, the adaptive law:

$$(z_4 - z_{4d})z_{5d} + (z_5 - z_{5d})z_{5d} + \frac{1}{\gamma}\dot{\tilde{\theta}} = 0 \tag{52}$$

Using the above equation and the fact that $\dot{\tilde{\theta}} = \dot{\hat{\theta}}$, the adaptive law will be:

$$\hat{\theta} = \hat{\theta}_1 + \hat{\theta}_2 = -\int\left[(z_4 - z_{4d})z_{4d} + (z_5 - z_{5d})z_{5d}\right]dt \tag{53}$$

Under this condition

$$\dot{H}_d(t) = -\tilde{z}^T R_d \tilde{z} \le -\alpha H_d(t) \tag{54}$$

Where α is the strictly positive constant.

It is concluded that the error dynamics (48) are asymptotically stable towards the equilibrium point located at $z_{4d} = z_{5d} = V_d$.

Thus, in order to obtain desired error dynamics, and comparing (44), (48):

$$\psi = E - M\ \dot{z}_d - T\ (u) z_d - R z_d + R_a \tilde{z} \tag{55}$$

Using (41), (52) supposed:

$$\begin{aligned} &\psi = \begin{bmatrix} 0 & 0 & 0 & \tilde{\theta}_1 z_{4d} & \tilde{\theta}_2 z_{5d} \end{bmatrix}^T \\ &,\ \tilde{\theta}_1 = \hat{\theta}_1 - \frac{1}{R_L},\ \tilde{\theta}_2 = \hat{\theta}_2 - \frac{1}{R_L} \end{aligned} \tag{56}$$

Equation (55) is extended to the following scalar differential equations:

$$V_{FC} - L_{FC}\dot{z}_{1d} - r_{FC} z_{1d} - (1 - u_{FC}) z_{4d} + r_{a1}(z_1 - z_{1d}) = 0 \tag{57}$$

$$V_{Bat} - L_{Bat}\dot{z}_{2d} - r_{Bat} z_{2d} - (1 - u_{Bat}) z_{5d} + r_{a2}(z_2 - z_{2d}) = 0 \tag{58}$$

$$-L_{DC}\dot{z}_{3d} + z_{4d} - z_{5d} = 0 \tag{59}$$

$$-C_{FC}\dot{z}_{4d} + (1 - u_{FC}) z_{1d} - z_{3d} = (\hat{\theta}_1 - \frac{1}{R_L}) z_{4d} \tag{60}$$

$$-C_{Bat}\dot{z}_{5d} + (1 - u_{Bat}) z_{2d} + z_{3d} - \frac{z_{5d}}{R_L} = (\hat{\theta} - \frac{1}{R_L}) z_{5d} \tag{61}$$

The control objective of this study is the adaptive passivity-based control of DC output voltage, but the direct control is not feasible due to its lack of stability, see [38], hence, the indirect control is used for the regulation of output DC voltage to a constant equilibrium value.

Consider the equations of the boost DC/DC converter of fuel cell (57) and (60), the desired constant value for the fuel cell current (converter input current) is z_{1d}, from the first equation (57), the control variable u_{FC} can be solved as:

$$u_{FC} = 1 - \frac{1}{z_{4d}}\left[V_{FC} - r_{FC} z_{1d} + r_{a1}(z_1 - z_{1d})\right] \tag{62}$$

Substituting (62) into the Eq. (60), after a straightforward calculation, the controller state, $z_{4d}(t)$, can be achieved as:

$$\begin{aligned} \dot{z}_{4d} &= \frac{1}{C_{FC}}\left[\begin{aligned} &-z_{3d} - (\hat{\theta}_1 - \hat{\theta}) z_{4d} \\ &+ \frac{z_{1d}}{z_{5d}}\left(V_{FC} - r_{FC} z_{1d} + r_{a1}(z_1 - z_{1d})\right) \end{aligned}\right] \\ \dot{\hat{\theta}}_1 &= -\gamma(z_4 - z_{4d}) z_{4d} \end{aligned} \tag{63}$$

Also, consider the equations of DC/DC converter of battery storage (58) and (61), the desired constant value for the battery current is z_{2d}, the control variable u_{Bat} can be solved from the second equation as:

$$u_{Bat} = 1 - \frac{1}{z_{5d}}\left[V_{Bat} - r_{Bat} z_{2d} + r_{a2}(z_2 - z_{2d})\right] \tag{64}$$

Then substituting the control variable u_{Bat} into the Eq. (61), yields the controller state, $z_{5d}(t)$,

$$\begin{aligned} \dot{z}_{5d} &= \frac{1}{C_{Bat}}\left[\begin{aligned} &z_{3d} - \hat{\theta}_2 z_{5d} \\ &+ \frac{z_{2d}}{z_{5d}}\left(V_{Bat} - r_{Bat} z_{2d} + r_{a2}(z_2 - z_{2d})\right) \end{aligned}\right] \\ \dot{\hat{\theta}}_2 &= -\gamma(z_5 - z_{5d}) z_{5d} \end{aligned} \tag{65}$$

Calculation of controller states, $z_{4d}(t)$ and $z_{5d}(t)$, depends on z_{3d}, which can be achieved as:

$$\dot{z}_{3d} = \frac{1}{L_{DC}}\left[z_{4d} - z_{5d}\right] \tag{66}$$

V. Linear PI Controller Design

Design of PI controller is achieved based on average model of converters. Then, the linearized model of converter around an equilibrium points is used for design of PI controllers (see [39] for more details).

Suppose the boost converter in Figs. 4 and 5. (The subscripts of converter elements are not considered in the following equations).

$$L\frac{di_L}{dt} = E - r i_L - (1 - u) v_C \tag{67}$$

$$C\frac{dv_C}{dt} = (1 - u) i_L - i_O \tag{68}$$

Where L, C and r are respectively the inductance, capacitance and series equivalent resistance of inductor values of the circuit components. E and i_O are the constant value of the external voltage source and the output load current, respectively. u is control signal of converter.

With choosing the following variables:

$$z = \begin{bmatrix} z_1 & z_2 \end{bmatrix}^T = \begin{bmatrix} i_L & v_C \end{bmatrix}^T \quad (69)$$

Considering a desired output voltage $z_{2d} = V_d$, the other equilibrium point parameters will be:

$$z_{1d} = \frac{1}{2r}(E - \sqrt{E^2 - 4ri_O V_d}),\ u_d = 1 - \frac{E}{V_d} \quad (70)$$

Defining the following error variables

$$\tilde{z}_1 = z_1 - z_{1d},\ \tilde{z}_2 = z_2 - z_{2d},\ \tilde{u} = u - u_d \quad (71)$$

The linearized model is written as:

$$\dot{\tilde{z}} = A\tilde{z} + Be + F\tilde{u} \quad (72)$$

Where e, A, B and F are given by:

$$e = \begin{bmatrix} E \\ i_O \end{bmatrix},\ A = \begin{bmatrix} -\frac{r}{L} & -\frac{u'_d}{L} \\ \frac{u'_d}{C} & 0 \end{bmatrix},\ B = \begin{bmatrix} \frac{1}{L} & 0 \\ 0 & -\frac{1}{C} \end{bmatrix},$$
$$F = \begin{bmatrix} -\frac{z_{2d}}{L} \\ -\frac{z_{1d}}{C} \end{bmatrix} \quad (73)$$

Where u'_d is $1 - u_d$. After simple calculation demonstrated this system is controllable. Frequency response method for design of PI linear controllers has been used [40]. The controller of boost converter of fuel cell and battery storage is $G_{C\_PV}(s) = 0.001 + \frac{0.076}{s}$, $G_{C\_Bat}(s) = 0.002 + \frac{0.025}{s}$, respectively.

VI. Power Management System

In the proposed hybrid DC power source, the fuel cell and battery storage have cooperation to supply the load. Hence, the power management system needs to control the power flow between the fuel cell, battery and load.

The power management system acts based on certain strategies. In this study, the PMS strategies have been considered as:

- The fuel cell is the main source to supply power to the load.
- The battery storage is a backup source to supply transient power and peak load demands. Moreover, battery storage feeds the load when the load is more than the fuel cell power rating.
- The battery storage is charged by the fuel cell when the load power is less than the fuel cell rated power.

According to the above-mentioned strategies, the PMS algorithm is shown in Fig. 6.

In the proposed power management system: P_{Load}, P_{FC_rated}, P_{FC_gen}, P_{Bat} and P_e are load power, fuel cell rated power, fuel cell generated power, battery storage power, and power calculated based on subtraction between fuel cell rated power and load power, respectively.

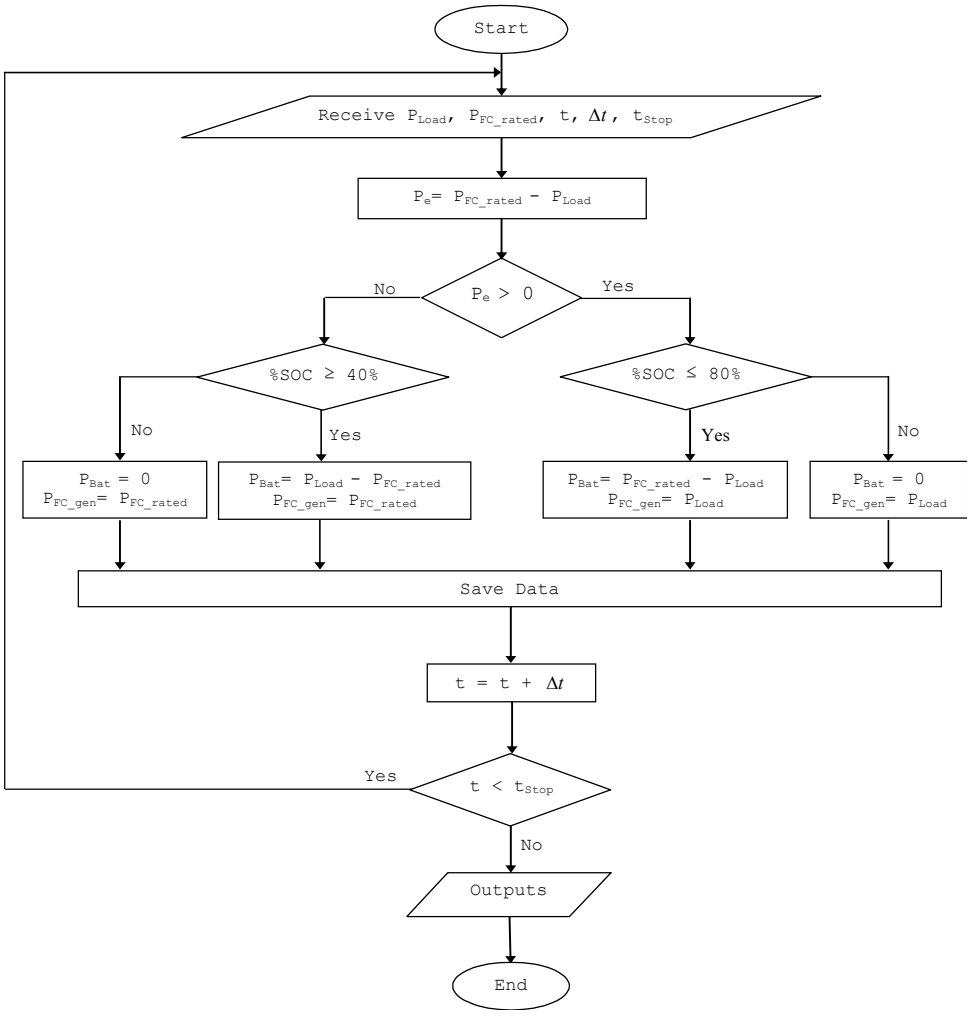

Fig. 6. Proposed power management system algorithm.

VII. Simulation Results and Discussion

The propose of this paper is to address the Euler-Lagrange framework modeling and adaptive passivity-based control of FC/Battery hybrid power source. MATLAB/Simulink environment is used to investigate the performance of the adaptive passivity-based control on FC/Battery hybrid power source. The mathematical model of each component in the DC hybrid power source has been presented in the previous sections. It consists of dynamic model of fuel cell Stack, dynamic model of Li-ion battery, nonlinear models of DC/DC boost converter and bidirectional DC/DC converter, adaptive passivity-based controllers and power management system. The specifications of SR-12 fuel cell Stack is shown in Table I. The specifications of Li-ion battery storage are given in table II. The DC/DC converters specifications are given in Table III.

These simulations are achieved in the two cases:

I. The DC bus voltage reference is constant; moreover the initial SOC% of the battery storage is 70 (first case).
II. The DC bus voltage reference changes; the initial SOC% of the battery storage is 85 (second case).

The rated power of PEM fuel cell is 500 watt.

A. First Case

The step change in resistive load is given in Fig. 7a. The DC bus voltage reference is 100 Volt. The system response to change in resistive load is presented in the following Figs. The load voltage (V_{DC}) and current (I_o) are shown in Figs. 7b and 7c.

APBC and PI controllers demonstrate to this fact that the adaptive passivity-based controller exhibits a smooth and fast transient to a step change in the resistive load.

In this case, the fuel cell has a maximum power generation, therefore, its voltage and current is a constant.

The battery storage voltage (V_{Bat}) and current (I_{Bat}) are shown in Figs 8a and 8b. According to PMS algorithm, the battery storage supply load in the transient conditions. Also, it supplies the remained load power when the load power is more than the fuel cell power rating.

TABLE I. SPECIFICATIONS OF PEM FUEL CELL (SR-12) [1]

Parameter	Value	Parameter	Value
$A\ (cm^2)$	62.5	$\eta_0(V)$	20.145
$P_{O2}\ (atm)$	1.0	$P_{H2}\ (atm)$	1.5
$a\ (VK^{-1})$	-0.1373	$b\ (VK^{-1})$	$7.48.10^{-5}$
$B\ (V)$	0.15	$l\ (m)$	25.10^{-6}
n_s	48	$R_C\ (ohm)$	0.0003
$J_{max}\ (mAcm^{-2})$	672	$C\ (F)$	4.8
$R\ (Jmol^{-1}K^{-1})$	8.3143	$F\ (Coulom^{-1})$	96487

TABLE II. SPECIFICATIONS OF LI-ION BATTERY [41]

Parameter	Value
Capacity (mAh)	850
Nominal Voltage (V)	3.7
Max. Charge Voltage (V)	4.23
Number of series Cell	12
Number of parallel strings	4

TABLE III. SPECIFICATIONS OF DC/DC CONVERTERS

Parameter	Value	Parameter	Value
$L_{FC}(mH)$	23.2	$L_{Bat}(mH)$	37
$C_{FC}(\mu F)$	330	$C_{Bat}(\mu F)$	470
$r_{FC}\ (\Omega)$	0.03	$r_{Bat}\ (\Omega)$	0.07

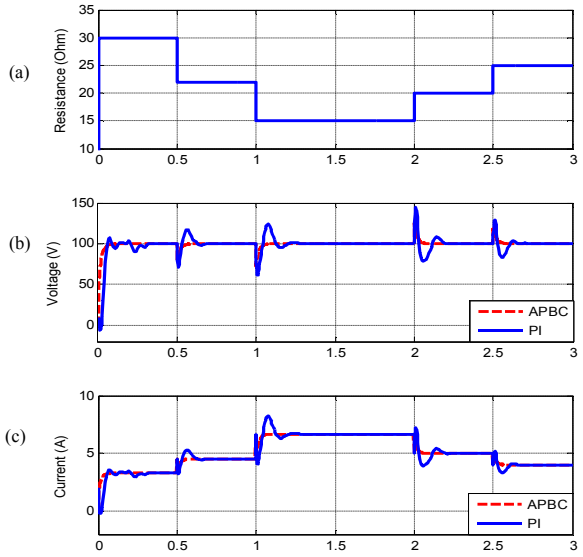

Fig. 7. (a) Load resistance, (b) DC bus, Load voltage and DC bus voltage reference and (c) Load current.

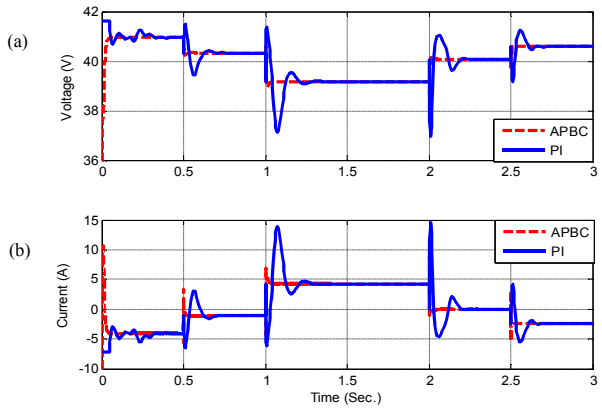

Fig. 8. Battery storage: (a) voltage and (b) current.

The battery storage voltage and current based on adaptive Passivity-based controller has lower overshoot than linear PI controller, and these also settle to the steady-state value faster. The SOC of battery storage with utilization of both controllers is shown in Fig. 9a. It is evident that the fluctuations on SOC based on PI controller are more than APB Controller.

The estimated value of resistance is shown in Fig. 9b which demonstrates that the estimated value converges very close to the true values. Similar results with aforementioned cases have been presented in [33] for adaptive passivity-based control of boost DC/DC converter. Also the results of quasi-resonant converter control via adaptive passivity-based control have been documented in [42] which demonstrate to verity of this study results.

In this case, the initial SOC% of battery storage is 70. Therefore, battery storage is in the discharge mode between (t=1 and t=2 sec). Because the load power exceeds from the fuel cell power rating, the generated power of fuel cell is maximum. That is evident in Figs. 10a and 10b for APBC and PI, respectively. The flowed power based on APBC has a short settling time, low overshoot and zero steady-state error towards PI controller.

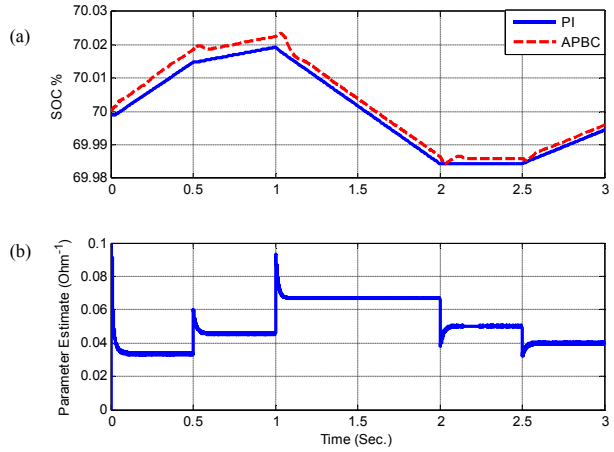

Fig. 9. (a) SOC of battery storage and (b) Estimated value of $1/R_L$.

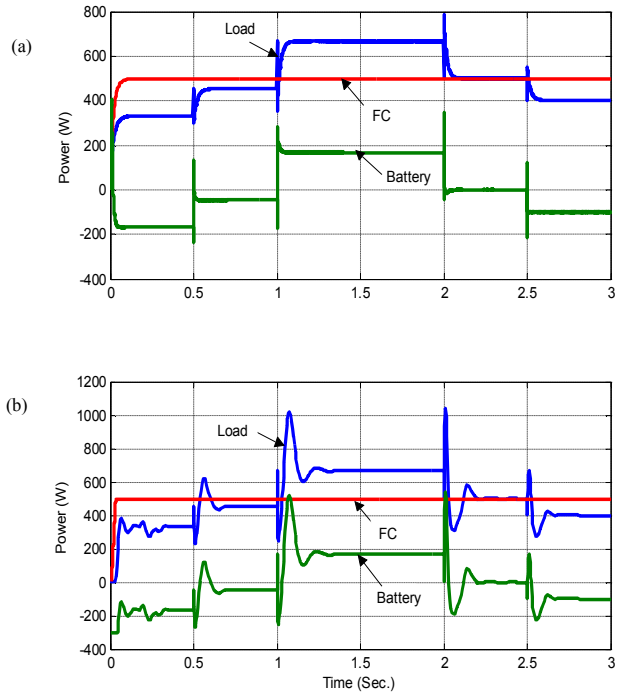

Fig. 10. Load, FC and battery power: (a) APBC and (b) PI.

B. Second Case

In the second case, the DC bus reference is not constant. Also, the initial SOC% of battery is 85. The step change in the resistive load is given in Fig. 11a.

Fig. 11b presents the system response to change in the DC bus voltage reference and load resistance. The load voltage (V_{DC}) based on APBC tracks well the voltage reference. Also, it is observed a zero steady-state error and a short settling time towards PI controller responses. The load current (I_o) is shown in Fig 11c.

The fuel cell voltage (V_{FC}) and current (I_{FC}) are shown in Figs. 12a and 12b. It has a rated power generation (between t=0.5 and t=1.5 sec, t=2.5 and t=3sec).

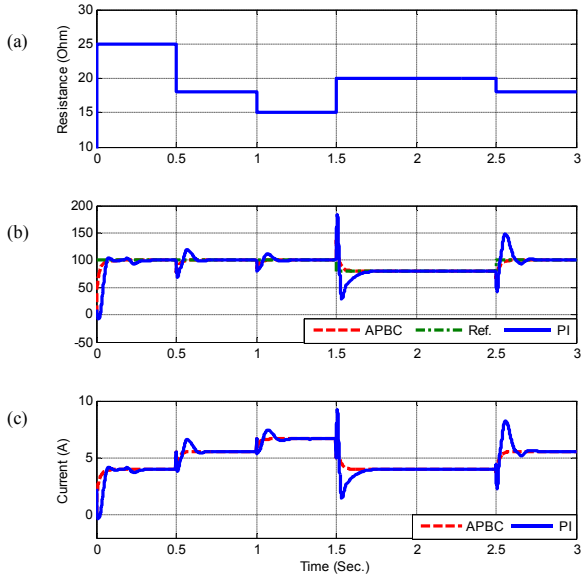

Fig.11. (a) Resistance load, (b) DC bus, Load voltage and DC bus voltage reference and (c) Load current.

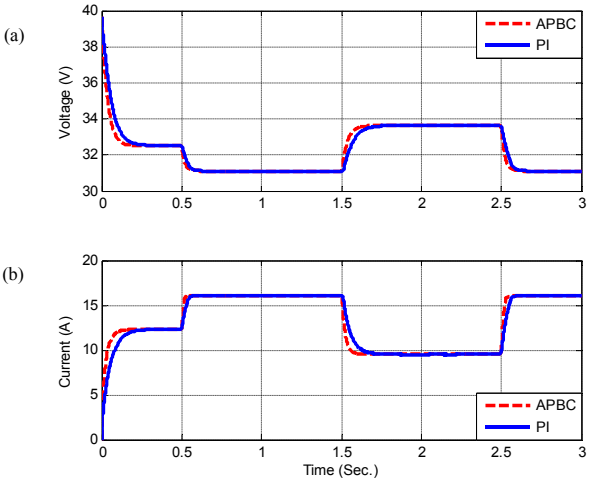

Fig.12. Fuel cell: (a) voltage and (b) current.

The fuel cell voltage and current has a smooth behavior towards resistive load and DC reference voltage changes. SOC% of the battery storage has been limited between 40 and 80. Therefore, based on PMS algorithm, it has no charging mode in this case. Figs. 13a and 13b present the battery storage voltage (V_{Bat}) and current (I_{Bat}). According to mentioned Figs., the battery voltage and current based on APBC a low overshoot and zero steady-state error are observed towards the linear PI controller.

The power flow between components is shown in Figs. 14a and 14b for APBC and PI controller, respectively.

In this case, the battery storage is not on safe charge mode. Also, the battery storage supplies the transient power and the excess power of load which is more than rated power of fuel cell. The better performance of APBC towards the PI controller is observed with a short settling time and a zero steady-state error on flowed power.

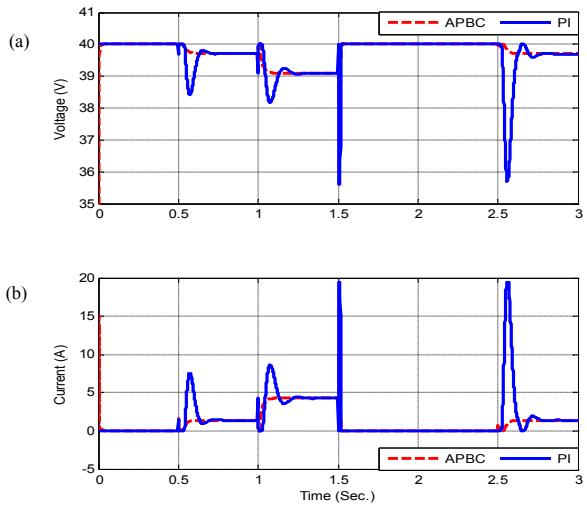

Fig.13. Battery storage: (a) voltage and (b) current.

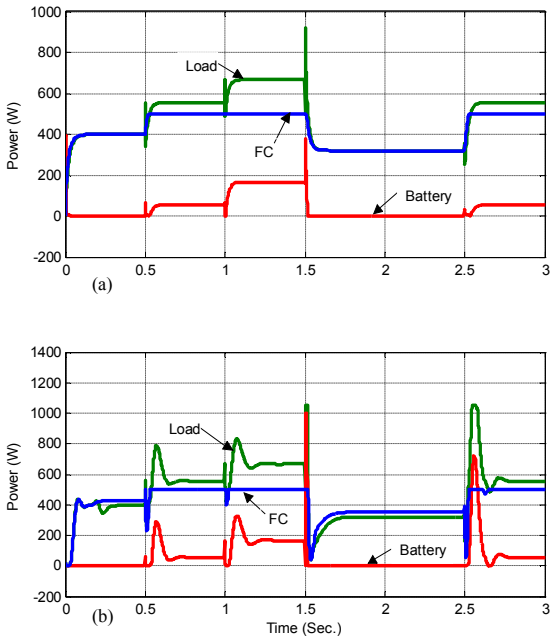

Fig.14. Load, FC and battery power: (a) APBC and (b) PI.

In this study, it can be seen that the hybrid power source with the proposed controllers is robust towards resistive load and DC bus voltage reference changes.

VIII. CONCLUSION

In this paper, the Lagrangian modeling of a hybrid DC power source composed of a PEM fuel cell as main source, Li-ion battery storage as transient source and interfacing DC/DC converters have been presented. Subsequently, according to energy shaping and damping injection method, adaptive passivity-based controllers have been designed to control the interfacing DC/DC converters. Control of power flow between components has been done in the power management unit. The linear controllers have been provided for investigation of proposed system validity.

The proposed model has been validated by simulation results. Two cases have been studied, constant DC bus voltage reference and SOC%=70%, in this case, the battery storage, based on the load power situation, has cooperation to supply power to the load and absorb power from the fuel cell. In the second case, the DC bus voltage reference changes and SOC%=85%, therefore, the battery storage only supplies power to load.

In the outputs of hybrid system with proposed controllers are observed a low overshoot, a short settling time and a zero steady-state error towards PI controllers. The aforementioned results demonstrate the robustness of the proposed controllers in the resistive load and DC bus voltage reference changes.

REFERENCES

[1] C. Wang, M.H. Nehrir, S.R. Shaw, "Dynamic models and model validation for PEM fuel cells using electrical circuits, " IEEE Trans. on Energy Conversion, vol. 20 , Issue 2, pp. 442 – 451, 2005.

[2] Z. Jiang, R.A. Dougal, "A hybrid fuel cell power supply with rapid dynamic response and high peak-power capacity," Twenty-First Annual IEEE Applied Power Electronics Conference and Exposition, APEC '06, pp. 1250-1255, 2006.

[3] J.M. Andujar, M. Segura, J. Vasallo, "A suitable model plant for control of the set fuel cell DC/DC converter," Renewable Energy vol. 33, Issue 4, pp. 813-826, April 2008.

[4] SM Sharifi Asl, S. Rowshanzamir, M.H. Eikani, "Modelling and simulation of the steady-state and dynamic behavior of a PEM fuel cell," Energy, vol. 35, Issue 4, pp.1633-1646, April 2010.

[5] M.J. Khan, M.T. Iqbal, "Dynamic modeling and simulation of a small wind–fuel cell hybrid energy system," Renewable Energy, vol. 30, Issue 3, pp. 421-439, March 2005.

[6] M. Amirabadi, SH. Farhangi, "Fuzzy control of hybrid fuel cell/battery power source in electric vehicle," 1st IEEE Conference on Industrial Electronics and Applications, pp. 1-5, 2006.

[7] C. Wang, M.H. Nehrir, H. Gao, "Control of PEM fuel cell distributed generation systems," IEEE Trans. on Energy Conversion, vol. 21, Issue 2, pp. 586-595, 2006.

[8] M. Uzunoglu, M.S. Alam, "Dynamic modeling, design and simulation of a PEM fuel cell/ultra-capacitor hybrid system for vehicular applications," Energy Conversion and Management, vol. 48, Issue 5, pp. 1544-1553, May 2007.

[9] T.L. Skvarenina, "The power electronics handbook," USA: CRC Press, 2002.

[10] Z. Jiang, R.A. Dougal, "A compact digitally controlled fuel cell/battery hybrid power source," IEEE Trans. on Industrial Electronics, vol. 53, Issue 4, pp. 1094-1104, 2006.

[11] C-H Li, X-J Zhu, G-Y Cao, S. Sui, M-R Hu, "Dynamic modeling and sizing optimization of stand-alone photovoltaic power systems using hybrid energy storage technology," Renewable Energy, vol. 34, Issue 3, pp. 815-826, March 2009.

[12] M.T. Gencoglu, Z. Ural, "Design of a PEM fuel cell system for residential application," International Journal of Hydrogen Energy, vol.34, Issue 12, pp.5242-5248, June 2009.

[13] M.J. Khan, M.T. Iqbal, "Dynamic modeling and simulation of a fuel cell generator," Fuel Cells, vol. 5, Issue 1, pp. 97-104, 2004.

[14] M.Y. El-Sharkh, A. Rahman, M.S. Alam, A.A. Sakla, P.C. Byrne, T. Thomas, "Analysis of active and reactive power control of a stand-alone PEM fuel cell power plant," IEEE Trans. on Power Systems, vol. 19, Issue 4 , pp. 2022-2028, 2004.

[15] Y.H Li, S.S. Choi, S. Rajakaruna, "An analysis of the control and operation of a solid oxide fuel-cell power plant in an isolated system," IEEE Transactions on Energy Conversion, vol. 20, no. 2, pp. 381-387, 2005.

[16] O.C. Onar, M. Uzunoglu, M.S. Alam, "Dynamic modeling, design and simulation of a wind/fuel cell/ultra-capacitor-based hybrid power generation system," Journal of Power Sources, vol. 161, Issue 1, pp.707-722, October 2006.

[17] C. Batlle, A. Dòria-Cerezo, E. Fossas, "Bidirectional power flow control of a power converter using passive hamiltonian techniques," International Journal Circuit Theory Application, vol. 36, pp. 769–788, 2008.

[18] D. Cortés, J. Alvarez, J. Alvarez, "Robust Control of the Boost Converter," International Conference on Industrial Electronics and Control Applications," ICIECA, pp. 1-6, 2005.

[19] S.K. Mazumder, A.H. Nayfeh, D. Borojevic, "Robust control of parallel DC–DC buck converters by combining integral-variable-structure and multiple-sliding-surface control schemes," IEEE Trans. on Power Electronics, vol. 17, Issue 3, pp. 428-437, 2002.

[20] D-E Kim, D-C Lee, "Feedback linearization control of three-phase AC/DC PWM converters with LCL input filters," 7th International

Conference on Power Electronics, ICPE '07, pp.766-771, October 22-26, 2007.

[21] N. Vazquez, C. Hernandez, J. Alvarez, J. Arau, "Sliding mode control for DC/DC converters: A new sliding surface," IEEE International Symposium on Industrial Electronics, ISIE '03. pp. 422-426, 2003.

[22] R. Leyva, A. Cid-Pastor, C. Alonso, I. Queinnec, S. Tarbouriech, L. Martinez-Salamero, "Passivity-based integral control of a boost converter for large-signal stability," IEE Proceedings-Control Theory and Applications, vol. 153, Issue 2, pp. 139-146, 2006.

[23] R. Ortega, A. Van Der Schaft, B. Maschke, G. Escobar, "Interconnection and damping assignment passivity-based control of port-controlled hamiltonian systems," Automatica, vol. 38, Issue 4, pp. 585-596, April 2002.

[24] R. Ortega, A. Loria, P. J. Nicklasson, H. Sira-Ramirez, "Passivity based Control of euler-lagrange systems: mechanical, electrical and electrochemical applications," London, U.K.: Springer-Verlag, 1998.

[25] J.M.A. Scherpen, D. Jeltsema, J.B. Klaassens, "Lagrangian modeling of switching electrical networks," Systems & Control Letters, vol. 48, Issue 5, pp. 365-374, April 2003.

[26] A. Dòria-Cerezo, "Modeling, simulation and control of a doubly-fed induction machine controlled by a back-to-back converter," PhD Destination, Technical University of Catalonia, 2006.

[27] A. Kwasinski, P.T. Krein, "Passivity-based control of buck converters with constant-power loads," IEEE Power Electronics Specialists Conference, PESC '07, pp. 259-265, 2007.

[28] P. Wang, J. Wang, Z. Xu, "Passivity-based control of three phase voltage source PWM rectifiers based on PCHD model," International Conference on Electrical Machines and Systems, ICEMS '08, pp. 1126-1130, 2008.

[29] T.S. Lee, "Lagrangian modeling and passivity-based control of three-phase AC/DC voltage-source converters," IEEE Trans. on Industrial Electronics, vol. 51, Issue 4, pp. 892-902, August 2004.

[30] H. Komurcugil, "Steady-state analysis and passivity-based control of single-phase PWM current-source inverters," IEEE Trans. on Industrial Electronics, vol. 57, Issue 3, pp. 1026-1030, March 2010.

[31] M.Y. Ayad, M. Becherif, A. Henni, A. Aboubou, M. Wack, S. Laghrouche, "Passivity-based control applied to DC hybrid power source using fuel cell and supercapacitors," Energy Conversion and Management, vol. 51, Issue 7, pp.1468–1475, 2010.

[32] H. Sira-Ramirez, M. Rios-Bolivar, A.S.I Zinober, "Adaptive dynamical input-output linearization of DC to DC Power converters: a backstepping approach," International Journal Robust and Nonlinear Control, vol. 7, pp. 279-96, 1997.

[33] H. Sira-Ramirez, R. Ortega, M. Garci-Esteban, "Adaptive passivity-based control of average DC-to-DC power converters models," International Journal Adaptive Control Signal Process, vol. 12, pp. 63-80, 1998.

[34] K.S. Jeong, W.Y. Lee, C.S. Kim, "Energy management strategies of a fuel cell/battery hybrid system using fuzzy logics," Journal of Power Sources, vol. 145, Issue 2, pp.319–26, 2005.

[35] S.A. Khateeb, M.M. Farid, J.R. Selman, S. Al-Hallaj, "Mechanical–electrochemical modeling of Li-ion battery designed for an electric scooter," Journal of Power Sources, vol.158, Issue 1, pp.673–678, 2006.

[36] M. Durr, A. Cruden, S. Gair, J.R. McDonald, "Dynamic model of a lead acid battery for use in a domestic fuel cell system," Journal of Power Sources, vol. 161, Issue 6, pp.1400–1411, 2006.

[37] M. Chen, G.A. Rinco'n-Mora, "Accurate electrical battery model capable of predicting runtime and I–V performance," IEEE Trans. on Energy Conversion,vol.21, Issue 2, pp. 504-511, 2006.

[38] G. Escobar, R. Ortega, H. Sira-Ramirez, J.P. Vilain, I. Zein, "An experimental comparison of several nonlinear controllers for power converters," IEEE Control Systems Magazine, vol. 19, Issue 1, pp. 66-82, 1999.

[39] R. W. Erickson. "Fundamentals of Power Electronics Instructor's slides," [Online]. Available: http://ecee.colorado.edu/~pwrelect /book/slides.

[40] R. Dorf, "Modern control system," Prentice Hall, 11nd Ed. August 10, 2007)

[41] Specifications of Polymer Lithium Ion Battery, Model: PL-383562.

[42] M. Becherif, M.Y. Ayad, A. Miraoui, "Modeling and passivity-based control of hybrid sources: fuel cell and supercapacitors," 41st IAS Annual Meeting Industry Applications Conference, pp. 1134-39, 2006.